atmosphere

MDPI

Article

Concept of Using an Unmanned Aerial Vehicle (UAV) for 3D Investigation of Air Quality in the Atmosphere—Example of Measurements Near a Roadside

Abdul Samad *, Diego Alvarez Florez, Ioannis Chourdakis and Ulrich Vogt

Department of Flue Gas Cleaning and Air Quality Control, Institute of Combustion and Power Plant Technology (IFK), University of Stuttgart, Pfaffenwaldring 23, 70569 Stuttgart, Germany; st109736@stud.uni-stuttgart.de (D.A.F.); ioannis.chourdakis@ifk.uni-stuttgart.de (I.C.); ulrich.vogt@ifk.uni-stuttgart.de (U.V.)

* Correspondence: abdul.samad@ifk.uni-stuttgart.de

Abstract: A substantial amount of air pollution is emitted from urban sources. Hence, investigating air pollutant dispersion from urban sources is of great importance. The mechanisms influencing air pollutant dispersion also need to be studied thoroughly. Unmanned Aerial Vehicle (UAV)-based systems offer great potential for mobile exploration of air pollutants in the lower atmosphere due to the high maneuverability of multi-rotor UAVs. The aim of this study was to develop an effective UAV system that can perform high-resolution three-dimensional profiling of pollutants, such as particulate matter (PM), ultrafine particles (UFP), black carbon (BC), as well as meteorological parameters, including air temperature, relative humidity, pressure, wind speed, and wind direction. Different experiments were performed to finalize the positioning of the instruments on the UAV platform so as not to destabilize the drone during flight, even when the wind speed is high and during turbulent flight conditions. Another very crucial question is where to place the air inlet of the measurement devices. In addition, field tests were conducted to evaluate the stability of the UAV platform and the in-flight performance of the sensors. This UAV platform was deployed to perform vertical profiles at the University campus in Stuttgart-Vaihingen and in an area near the campus, close to the federal highway B14. The measurement campaign was performed on three days in February 2021, with a maximum flight height of 120 m above ground. The vertical profiles showed that concentrations were higher on the ground due to the proximity to the source and that high wind speeds assisted pollutant dispersion. The horizontal profiles showed that the pollutant concentrations were higher at the roadside and decreased with increasing distance from the road. In conclusion, this UAV platform represented a low-cost, practical, and reliable method for studying the three-dimensional distribution of pollutants near the source.

Keywords: drone measurements; Unmanned Aerial Vehicle; vertical profiles; air pollution monitoring; air quality

check for updates

Citation: Samad, A.; Alvarez Florez, D.; Chourdakis, I.; Vogt, U. Concept of Using an Unmanned Aerial Vehicle (UAV) for 3D Investigation of Air Quality in the Atmosphere—Example of Measurements Near a Roadside. *Atmosphere* **2022**, *13*, 663. https://doi.org/10.3390/atmos13050663

Academic Editors: Jianbang Xiang, Tianjun Lu and Yisi Liu

Received: 17 March 2022
Accepted: 20 April 2022
Published: 21 April 2022

Publisher's Note: MDPI stays neutral with regard to jurisdictional claims in published maps and institutional affiliations.

Copyright: © 2022 by the authors. Licensee MDPI, Basel, Switzerland. This article is an open access article distributed under the terms and conditions of the Creative Commons Attribution (CC BY) license (https://creativecommons.org/licenses/by/4.0/).

1. Introduction

Air pollution in cities has gained great concern in recent years as it threatens the health of millions of people. As stated by the World Health Organization (WHO), more than 80% of people living in urban areas that monitor air pollution are exposed to air quality levels that exceed the WHO recommendations. Traffic-related air pollution (TRAP) is considered to be the cause of a wide range of adverse human health effects as well as one of the main sources of pollution in urban areas [1,2]. Most of the world population is regularly exposed to TRAP due to daily activities (e.g., commuting) and to the fact that a significant number of people live near major roadways. Traffic-induced emissions are higher near roads but drop significantly within a distance of a few hundred meters [3]. Different factors affect the variation gradients, such as traffic conditions, topography, temperature, relative

humidity, wind speed, wind direction, atmospheric stability, and mixing layer heights [4]. There are many methods available to investigate the pollutant dispersion along roadsides, for instance, vehicle-based mobile platforms, statioary monitoring stations, and portable devices. However, most of these methods provide assessments of ground-level pollutant profiles. In order to obtain a complete picture of pollutant dispersion and the impact of traffic emissions, both vertical and horizontal profiles are required.

A portable air quality measurement system is therefore required to study the spatial dispersion of air pollutants and their impact on air quality. The method developed in this study uses lightweight, precise sensors and a battery-powered hexacopter UAV, the maneuverability and flexibility of which allows high-resolution sampling near the source. Compared to other conventional methods, such as meteorological towers, tethered balloon systems, and manned aircrafts, this UAV-based method can perform three-dimensional measurements, even at low altitudes, and can be easily transported and prepared at the measurement location.

This research focused on developing a UAV platform capable of performing reliable measurements of particulate matter (PM), ultrafine particles (UFP), black carbon (BC), and meteorological parameters, such as air temperature, relative humidity, pressure, and wind speed and direction. An investigation regarding the influence of the airflows caused by the propellers on the air distribution around the hexacopter UAV was also performed using a colored smoke column.

2. Present State of Knowledge

The emission sources producing air pollutants are both natural and anthropogenic. Natural emission sources include emissions from vegetation, deserts, volcanoes, and wildfires, while anthropogenic emission sources are produced mainly from power plants, domestic heating, industrial production, and transportation. The later has a higher impact on health and the environment [5]. Currently, ambient air pollutant concentrations are measured by stationary monitoring stations, which are often considered insufficient to cover large areas and are often unable to perform direct measurements at a source due to the complexity of sites, moving sources, or physical barriers (e.g., plumes emitted by combustion processes, such as those occurring in trucks, ships or industrial stacks) [6].

On the one hand, vehicle-based air quality monitoring systems have improved spatial coverage and can be used for source classification. Nevertheless, these applications can be limited by location, proper orientation to the source (e.g., upwind vs. downwind), complex topography, or transportation, and highly sensitive equipment is required. Furthermore, three-dimensional measurements (vertical profiles and horizontal profiles above ground level) are required to provide high spatial and temporal resolution for air quality data. This has been achieved previously by using towers, aircrafts, tethered balloons, and UAVs. The measurements using a tower are independent of measurement duration and allow for the comparison of measurement devices and offer more mounting space. However, the drawbacks include low vertical resolution, measurement height, and mobility [7]. Aircraft are mainly used to perform measurements at the altitude range of about 1–10 km, with an obligatory minimum flight height of 300 resp. 150 m. Tethered balloon systems do not require a minimum flight altitude, which allows the study of the vertical distribution of pollutants in the atmosphere from directly above ground [8]. However, tethered balloons cannot perform horizontal measurements, incur a significant cost, and require a long preparation phase. Multi-rotor UAVs, by contrast, represent an economical solution for investigating the lower atmosphere. They have become an attractive experimental platform for high-spatial resolution, near-surface, three-dimensional profiling of atmospheric pollution, as they can move in both horizontal and vertical dimensions and are able to hold their positions even under high-wind conditions [9].

With the rapid development of drone technology, UAV-based solutions for air quality monitoring have substantially increased in recent years. Researchers have already carried out atmospheric measurements using multi-rotor UAVs with onboard sensors and devices.

In 2016, a research group conducted a three-day measurement campaign in February, March, and April in Australia [10]. The Particle Number Concentration (PNC) vertical profiles adjacent to a motorway were measured by mounting a Mini Diffusion Size Classifier (DISCmini) from the Testo Company onboard a DJI S800 hexacopter UAV. During this study, flights were performed for about 12 to 15 min with a drone vertical speed between 1.5 and 2 m/s and a vertical height of 5 to 100 m. It was found that the PNC did not vary significantly at heights above 35 m, which suggested that emissions from vehicles on motorways did not directly affect the environment above this height. On the other hand, another study used a UAV platform to perform vertical profile measurements for monitoring BC concentrations during the winter season in the center of Warsaw and in a surrounding town. A strategy of fast ascent and low descent was applied in order to achieve a high spatial resolution and a long vertical profile. The BC concentration measurements were carried out with an Aethalometer AE51 (AethLabs) on a Versa X6sci hexacopter UAV. Their results verified the direct influence of temperature inversion on BC concentrations [11].

A study performed in a rural site of Northern China developed a novel setup to measure the vertical profile of particle number size distribution (PNSD) and meteorological parameters using an Awing-X40 Quadrant Space (Tianjin) hexacopter UAV equipped with a custom-built scanning mobility particle sizer (Hy-SMPS), an optical particle counter (Hy-OPC), and air temperature and relative humidity sensors. This setup was used to investigate the vertical profiles of air temperature, relative humidity, and PNSD, from the ground up to 300 m above ground level (AGL). The results showed that the PNSDs (8–25 nm in diameter) at 300 m AGL were higher than those on the ground level and that the formation of new particles was vertically inhomogeneous [12]. Another study in China conducted a measurement campaign of 23 days during February and March 2018. The flights were carried out at a fixed time, between 05:00 to 06:00 a.m. local time (LT), as the boundary layer is usually lower before sunrise such that it was more likely that the characteristics of PM pollutants within the whole boundary layer would be revealed. Vertical flights were performed from the ground up to 500 m AGL at a constant ascent speed of 1 m/s, hovered at the peak for 20 s, and then descended along the same path at the same speed. The payload module with a DustTrak^{TM} II Aerosol Monitor 8530 (TSI, Shoreview, MN, USA), an Aethalometer AE51 (AethLabs, San Francisco, CA, USA), and a Q-TRAK^{TM} 7595 (TSI), was mounted below a DJI Matrice 600 hexacopter UAV for conducting PM2.5 and BC measurements and air temperature and relative humidity measurements. All the inlets of the instruments were placed 20 cm above the drone to minimize the influence of the downwash effect. The results reveal that, overall, PM2.5 and BC concentrations decreased with height and, apart from local emissions, meteorological parameters along with regional transport may play important roles in PM2.5 and BC vertical profiles [13].

Finally, a research group conducted a measurement campaign near to an elevated highway in China. A DJI Matric 600 hexacopter UAV was equipped with portable sensors (a DustTrak^{TM} DRX Aerosol Monitor 8534 TSI, an Aethalometer AE51 (AethLabs), and an Onset HOBO U12-013 Data Logger (Onset Computer, Bourne, MA, USA)) to monitor PM, BC, relative humidity, and air temperature. The vertical flight of 0–500 m was carried out at two locations. Horizontally, the flight route involved two directions perpendicular to the road. During the experimental campaigns, the traffic volumes and composition were recorded using a high-definition camera and an infrared camera mounted on the drone and then manually counted. From the results, it was concluded that road configurations have important effects on the diffusion of the measured pollutants. All the pollutants dropped to lower concentration levels after 100 m horizontally. However, at the location with the more complicated road configuration, the distance exceeded 200 m [7].

The strong downwash flow generated by the propellers of multi-rotor UAVs is the biggest drawback when using UAVs as platforms for atmospheric pollutant sensing. The downwash flow has a significant influence on the air distribution around the UAV, which can alter the measurements by the on-board sensors. Therefore, to avoid the influence

of the rotating airflow field on the measurements, it is crucial to determine the optimum position for the sensor air intakes. Until now, several methods have been used to study the aerodynamic characteristics of multi-rotor UAVs. A research group used Computational Fluid Dynamics (CFD) simulations to describe the downwash flow field of a six-rotor UAV with similar features to the one used in this study. The results revealed that the shape of the airflows formed by the propellers is comparable to a cylinder, with the longest segment below the hexacopter UAV. Calculations of the magnitude of air velocity showed high values in the immediate vicinity of the propellers as well as below the propellers, whereas the corresponding values above the propellers were significantly lower. Therefore, the sensor air intakes must be placed above the propellers of the hexacopter UAV [14]. Concerning the minimum height of the air sensor intakes, two main visual airflow tests have been employed: using colored smoke plumes [15] and using tufts attached to a tube fixed above the multi-rotor UAV [12]. A range of heights (from 20 up to 150 cm) has been chosen for the placement of the sensor air inlets [7,12,13,16]. However, the downwash flow field of each multi-rotor UAV model is different and therefore must be studied individually.

The application of UAVs and low-cost sensors for air quality monitoring is increasing rapidly as many recent studies have applied this technique in various parts of the world. An interesting study involving a UAV platform equipped with economical air quality sensors was performed to monitor the air pollution emitted from waste in Lecce, Italy [17]. In Poland, a similar platform was used to monitor PM concentration in a municipal cemetery area in a suburban town [18]. Pollution maps were also generated using a UAV platform in a study performed by Alvear et al. The authors applied an algorithm to automatically monitor air pollution at higher concentrations [19]. Another study focusing on PM measurements using a low-cost PM sensor installed on a UAV platform was carried out at University Putra Malaysia [20].

3. Measurement Technique and Methodology

This section focuses on the methodology and measurement technique applied to develop the UAV platform that was designed to perform reliable three-dimensional measurements of air pollutants, such as particulate matter, black carbon, ultrafine particles, and meteorological parameters, such as temperature, relative humidity, pressure, wind speed, and wind direction.

3.1. Multi-Rotor UAV

The hexacopter DJI MATRICE 600 PRO that is shown in Figure 1 was selected as the carrier of this platform due to the flight performance, payload capabilities, and robust control system. The DJI MATRICE 600 PRO is equipped with a dedicated DJI™ A3 PRO (Guangdong, China) triple-modular redundancy system and advanced intelligent flight functions, ensuring safe and stable operation at all times. Its mechanical design with quick-release landing gears and mounted folding arms makes it easy to transport, store, and prepare for flight. According to the technical description, it has a maximum takeoff weight (including UAV) of 15.5 kg and uses six intelligent batteries to extend the flight time up to around 30 min without load or around 15 min with a 6 kg load.

3.2. Portable Sensors and Devices

In order to select the sensors and device to be mounted on the hexacopter UAV, several options were considered and compared according to their capability to perform reliable real-time measurements with respect to compactness, weight, size, cost, and battery time. The sensors and devices chosen for the air pollutants and meteorological parameters investigated in this study are discussed below.



Figure 1. DJI MATRICE 600 PRO Hexacopter UAV (photo courtesy of DJI).

3.2.1. OPC-N3

For measuring PM1, PM2.5, and PM10, a small and lightweight (105 g) optical particle counter (aerosol spectrometer) OPC-N3 from the company Alphasense was chosen. This low-cost PM sensor measures the particle number concentration with a measurement range of 0.35 until 40 µm distributed in 24 size classes. The OPC-N3 uses the light-scattering principle to measure particle size and particle number concentration. Particle mass loadings, PM1, PM2.5, and PM10, are then calculated from the particle size spectra and concentration data, assuming a particle density and refractive index (RI). Furthermore, the OPC-N3 uses a voltage-controlled fan to define the airflow through the measurement chamber in contrast to many other low-cost sensors that do not control the airflow at all [21]. The OPC-N3 requires a 4.8 to 5.2 Volt DC supply with minimal noise. Therefore, a data logger with an external Lipo Battery was added to the UAV platform for powering the OPC-N3 and acquiring data. In addition, the data logger combines the data from temperature and relative humidity sensors with the OPC's data and provides a timestamp for the single file. The OPC-N3 costs around EUR 350, making it a reliable low-cost sensor based on its performance compared to other low-cost sensors.

3.2.2. DISCmini (Testo)

The DISCmini (Diffusion Size Charger) was selected to measure the UFP number concentration since it is a small (180 × 90 × 42.5 mm), portable, lightweight (780 g), battery-operated monitor, which can measure PNC in the size range 10–700 nm at a fast time resolution of 1 s (1 Hz). The instrument measures total surface charge by charging aerosols electrostatically using a corona discharge. Then, it converts the measured charge and flowrate to concentration [22]. The DISCmini has been previously used for UAV applications and proven to be reliable for the investigation of the particle number concentration of UFPs [6,10].

3.2.3. AE51 (AethLabs)

This small (117 × 66 × 38 mm), lightweight (280 g), battery-operated, portable micro-aethalometer was used to measure BC concentration. The AE51 samples particles on a filter strip. A beam of light is directed on the spot of the particle-laden filter, and the attenuation of the transmitted light (wavelength: 880 nm) is recorded continuously. The optical absorption measured continuously is then converted to BC concentration [23]. The AE51 has been previously used in several studies and proven to be consistent with UAV applications [7,11,13].

3.2.4. TriSonica Mini Wind and Weather Sensor and Data Logger 222

A compact (91 × 91 × 52 mm), lightweight (50 g), 2D ultrasonic anemometer was chosen to measure primarily wind speed and wind direction. The open path provides the least possible distortion of the wind field. Four measurement paths provide redundant measurements. The path with the most distortion is removed from the calculations to provide accurate wind measurements. In addition, a battery-operated Data Logger 222 built into a weather-proof enclosure was acquired to power the TriSonica Mini and to collect and store its data. The Data Logger 222 was also adapted with a 433 MHz telemetry link to obtain real-time visualization of wind speed and wind direction values at the ground station.

3.2.5. iMet-XQ2 (InterMet)

The meteorological parameters, such as air temperature, relative humidity, and air pressure, along with geological information, were measured using an iMet-XQ2 sensor, which is a small (126 × 58 × 28 mm), lightweight (60 g), battery-operated atmospheric sensor. The iMet-XQ2 was selected due to its suitability for UAV applications and its ability to perform accurate measurements with high vertical resolution and precise spatial coordinates. Furthermore, this sensor can also be connected to the Data Logger 222, allowing the collection and transmission of data in real-time for all the meteorological parameters investigated in this study.

A summary of the portable sensors and devices mounted on the hexacopter UAV are listed in Table 1.

Table 1. Characteristics of the selected portable sensors and devices.

Parameter	Measurement Technique and Principle	Equipment Model (Manufacturer)	Measurement Range	Accuracy
		Air Pollutants		
PM1, PM2.5, and PM10	Optical Particle Counter (OPC) (Light Scattering)	OPC-N3 (Alphasense)	0.35–40 µm	-
Ultrafine Particles	Diffusion Charger (DC)	DISCmini (Testo)	10–700 nm	±500 #/cm^3
Black Carbon	Aethalometry (IR light absorption)	AE51 (AethLabs)	0–1 mg BC/m^3	±1 µg/m^3
		Meteorological		
Temperature Relative Humidity Pressure	Bead Thermistor Capacitive Piezoresistive	iMet-XQ2 (InterMet)	−90 to +50 °C 0–100% RH 10–2000 hPa	±0.3 °C ±5% ±1.5 hPa
Wind Speed Wind Direction	Ultrasonic Anemometer	TriSonica^{TM} Mini (Anemoment)	0–50 m/s 0–360°	±0.1 m/s ±1°

3.3. Downwash Effect Investigation with Smoke Test

The propellers of the UAV cause turbulence due to the downwash flow that can influence measurement results. It was believed that having the air inlet for the sensors and devices above a certain height of the UAV can solve this problem. In order to verify this and to determine the optimum height for the air inlet for the sensors and devices, a smoke test was performed in which a colored smoke plume about 5 m above ground level (AGL) was generated. The airflow around the UAV was examined at different heights of the air inlets above the UAV, as shown in Figure 2. In order to obtain a better visualization of the downwash flow influence on the smoke plume, a carbon fiber tube of 95 cm was placed above the rotor level and marked at 50 cm and 70 cm, as shown in Figure 2a. The length of the tube for this experiment was selected based on stability tests and supplier recommendations. Figure 2b shows that the influence of the vertical airflows on the smoke

column is practically negligible when the UAV hovers at about 90 cm below the smoke plume. However, once the UAV is slightly elevated at about 70 cm below the smoke plume, vertical airflows formed by the propeller begin to show an influence on the smoke column (Figure 2c). Figure 2d shows the effect of hovering the UAV slightly higher and perpendicularly closer to the smoke plume, at about 50 cm. In this position, the plume of smoke is further disturbed by the airflows caused by the propeller and the smoke is accelerated vertically downwards. This effect is observed predominantly towards the center of the UAV. Figure 2e shows that at about 30 cm between the smoke column and the propellers, the influence of the vertical airflows on the smoke plume increases and drifts to the windward side of the hexacopter UAV. However, once the hexacopter UAV reaches the same level of the smoke plume, the smoke is directly captured by the propellers and consequently dispersed downwards without passing throughout the hexacopter UAV, as seen in Figure 2f.

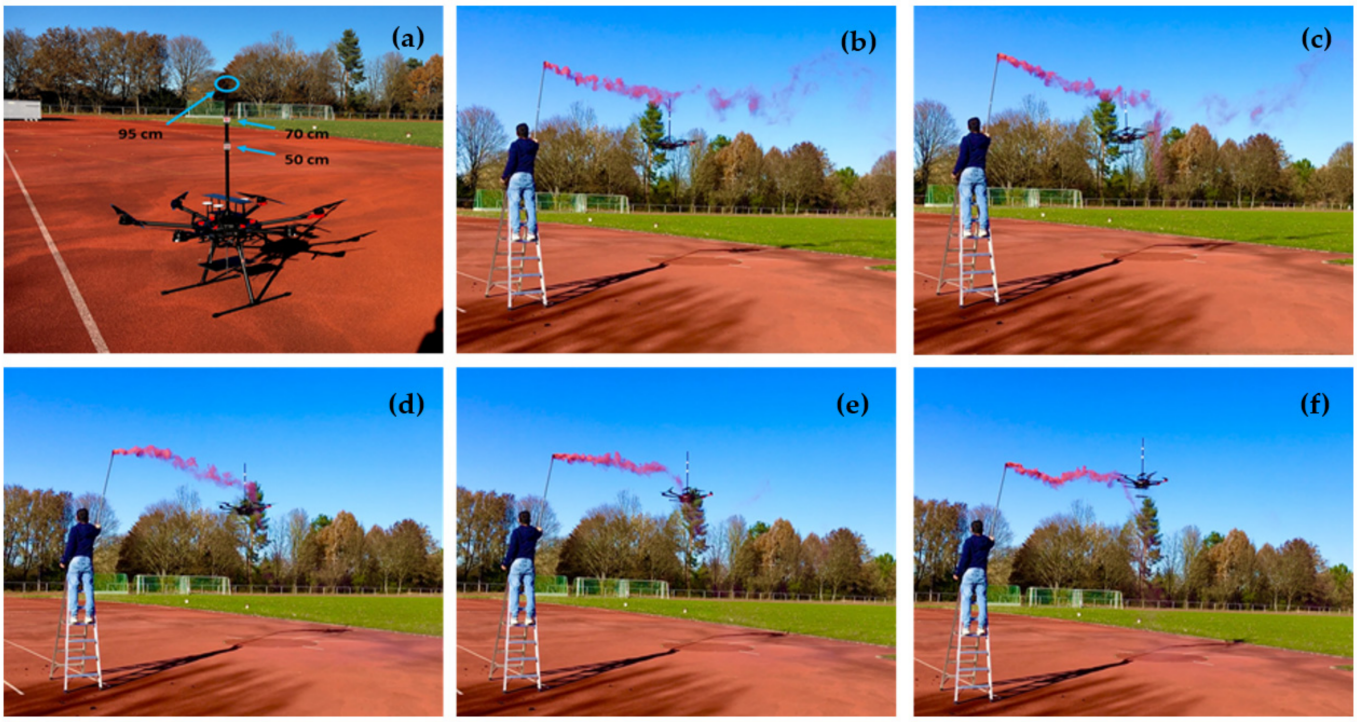


Figure 2. Investigation of the downwash flow caused by the propellers of the Hexacopter UAV (DJI M600 PRO) using a red colored smoke cartridge: (**a**) hexacopter UAV arrangement; (**b**) hexacopter UAV about 90 cm below the smoke plume; (**c**) hexacopter UAV about 70 cm below the smoke plume; (**d**) hexacopter UAV about 30 cm below the smoke plume; (**e**) hexacopter UAV about 30 cm below the smoke plume; and (**f**) hexacopter UAV at the same level of the smoke plume.

3.4. UAV Platform

The UAV platform is composed of: the hexacopter UAV, the sensor and portable devices, the inlet tubes, and two data loggers—one for the meteorological sensors and the other for the OPC-N3. The UAV platform with the propellers fully deployed measures 160 cm high and 170 cm wide and weighs 14 kg including all the measurement setup. The sensors and device, including the associated loads, weigh about 4 kg. In Figure 3, the configuration of the UAV platform is shown. A shelf of two levels was installed underneath the hexacopter UAV; the two data loggers and the external battery were placed on the higher level, and the AE51 and the DISCmini were placed on the lower level. Particularly for the DISCmini, careful positioning was essential in order to avoid possible stability issues. The smoke test showed that the influence of the downwash flow is negligible 90 cm above the propellers' level. Therefore, a 95 cm carbon fiber tube was fixed over the hexacopter UAV for mounting the TriSonica Mini and to support the sensor air intakes, which were

placed 90 cm above the hexacopter UAV. The OPC-N3 was strategically placed 60 cm above the hexacopter UAV on a base attached to the carbon fiber tube. In that way, the length of the inlet tube for the PM sensor was reduced from 90 cm to around 30 cm, improving the sampling accuracy. The XQ2 sensor was also placed above the hexacopter UAV, on the same base used for the OPC-N3. The atmospheric sensor was enclosed in a white plastic case to protect it from physical damage and avoid direct exposure of the temperature sensor to sunlight.

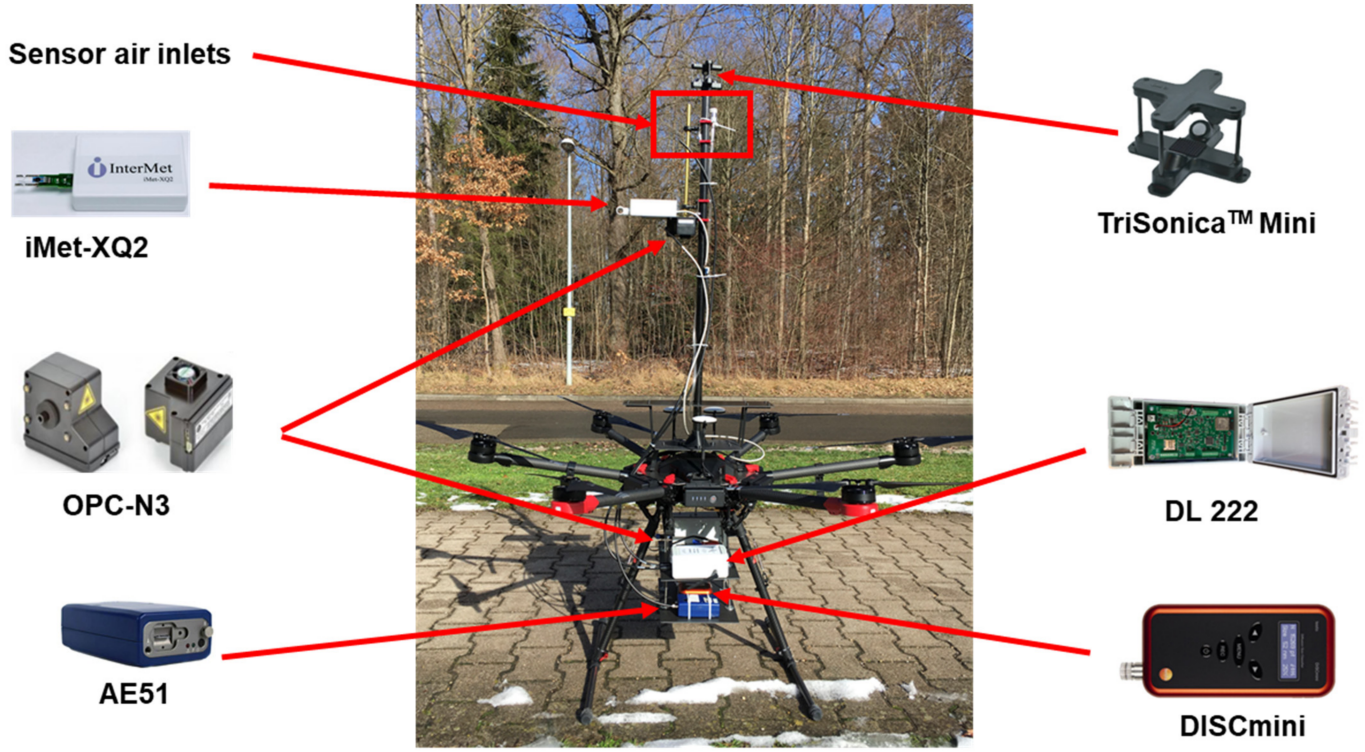


Figure 3. Configuration of the UAV platform.

3.5. Site Description

The field test was conducted next to the coal-fired power plant on the campus of the University of Stuttgart, in Stuttgart-Vaihingen (48.7506° N, 9.1103° E). As can be seen in Figure 4, the power plant is surrounded by university buildings and forest. The height of the power plant stacks located around 60 m AGL was used as a reference for the first experiments. The experiments for the case study were conducted in Am Lauchäcker next to the federal highway B14 with the purpose of studying the three-dimensional distribution of the traffic-related air pollutants and the influence of the meteorological parameters. Figure 5 shows the location of the measurement site (48°44′16.9″, N 9°05′51.0″ E). The take-off location, indicated with the red circle, was set up about 40 m north of the federal highway.



Figure 4. Google Earth image of the field test site showing the power plant of the University of Stuttgart-Vaihingen campus and the UAV take-off location (marked with the red circle).



Figure 5. Google Earth image of the case study measurement site Am Lauchäcker, showing the federal highway B14 and the UAV take-off location (marked with the red circle).

3.6. Experimental Procedure

The field test was carried out on 31 January 2021 due to favorable weather conditions: no rain, wind speed lower than 8 m/s, and wind coming from the east, which allowed us to catch the plant's emissions with the sensors on the hexacopter. Three vertical flights were

made using the UAV manual flight mode. The first flight consisted of a vertical ascent and descent from 0 to 100 m AGL. To obtain more representative measurements of the emission plume, the equipped UAV hovered for 1 min every 10 m between the heights of 40 and 100 m while ascending. Then, it was landed straight at the take-off location. The second flight consisted of two vertical flights, following the same procedure as in the first one, but instead of landing after the first vertical flight, the UAV platform was stopped at a height 40 m to start the second vertical flight and then landed directly at the take-off location. The measurement campaign took place on 16, 19, and 23 February 2021. The measurement days were selected taking into account specific weather conditions, such as no rain, wind speed values lower than 8 m/s, and wind coming from the south, so as to be able to measure the traffic emissions from the federal road B14. Table 2 shows the time schedule of the vertical and horizontal flights performed during the measurement campaign.

Table 2. Time schedule of the flights during the measurement campaign.

Day	Date	Start Time (LT)	Flight Mode	Height Range (m)
1	16 February 2021	13:20	Vertical	0–120
	16 February 2021	13:42	Vertical	0–120
	16 February 2021	13:52	Vertical	10–120
2	19 February 2021	13:46	Vertical	0–120
	19 February 2021	13:59	Vertical	10–120
	19 February 2021	14:10	Vertical	0–120
	19 February 2021	14:21	Vertical	10–120
3	23 February 2021	09:47	Vertical	0–120
	23 February 2021	11:14	Vertical	0–120
	23 February 2021	12:39	Vertical	0–120
	23 February 2021	12:10	Horizontal	30
	23 February 2021	13:41	Horizontal	30

The first two days were used to examine different vertical flight paths. On day 1, three vertical flights were performed using two different flight paths, starting from 0 up to 120 m AGL. During the first flight, the UAV platform hovered for 20 s every 10 m while ascending. Then it was landed directly at the take-off location. The second and third flights followed the same flight pattern. On day 2, four vertical flights were performed using two different flight patterns. In the first vertical flight, the equipped UAV hovered for 10 s every 10 m from the ground up to 120 m while ascending. Then it descended following the same pattern. The second vertical flight began at 10 m AGL. From there, the equipped UAV climbed up to 100 m at a nearly constant speed of about 1 m/s and then landed at the take-off point in the same way. The third and fourth vertical flights followed the same flight pattern as the first and second flights, respectively. On day 3, three vertical flights were made using the selected flight path, ascending and descending with stops of 10 s every 10 m, from the ground up to 120 m. Additionally, two horizontal flights were made at a height of 30 m in a parallel and perpendicular direction to the federal road B14.

Before conducting the flights, the time of all instruments was synchronized and the instruments were warmed up for at least 15 min. Time intervals for all instruments were set to one second. Additionally, the communication signal between the hexacopter UAV and the remote controller was verified to be completely stable. The barometric height formula [24] below was used to calculate the height above the ground. This describes how the pressure of the air changes with altitude.

$$h = h_b + \frac{T_b}{L_b} \cdot \left[\left(\frac{P}{P_b} \right)^{\frac{-R \cdot L_b}{g_0 \cdot M}} - 1 \right]$$

where:

h = the height at which pressure is calculated;
h_b = the height of reference level b;
T_b = the reference temperature;
L_b = the temperature lapse rate;
P = the pressure of the air;
P_b = the reference pressure;
R^* = the universal gas constant;
g_0 = the gravitational acceleration;
M = the molar mass of the air.

Given the reference values, the only two unknowns in the barometric height formula are the pressure of the air and the height. With the iMet-XQ2, precise values of the air pressure were measured continuously throughout the flights and then the corresponding altitudes were calculated.

4. Results and Discussion

The results of vertical profiles of the meteorological parameters and pollutants are discussed in this section. The UAV platform was initially tested in a more controlled location to verify: stability, maneuverability, power consumption, and whether the accuracy of the measurements was influenced by the movement and hovering of the hexacopter UAV.

4.1. Field Test Results

To analyze the data collected from the vertical measurements, the measured parameters were plotted against the height and compared with each other to obtain an overview of the air quality conditions. The vertical profiles represent the average values per meter and they were created based on the one-second values of each sensor, except for the profiles of the BC concentrations, which are presented as 30 s moving averages, in order to compensate for the high fluctuations of the AE51 in the one-second mode time resolution.

The vertical profiles presented in Figure 6 represent the average values per meter of the ascents carried out during the field test. The temperature profiles overall decreased with height and had larger variations below 40 m, especially during the earliest ascent. The relative humidity profiles, on the other hand, tended to increase with height but also showed greater variation below 40 m. The wind speed profiles showed fluctuations throughout the flights and the values were lower than 4 m/s. Regarding the wind direction profiles, the biggest variations were observed below 20 m. This might have been due to obstacles such as buildings and trees in the surroundings of the take-off location. Concerning the pollutants, the vertical profile of the ultrafine particles and the PM1 showed similar results; concentrations increased significantly above 80 m of height, while the PM2.5 and PM10 profiles showed concentration increases from lower heights. The BC measurement device was not used for this experiment.

The power plant was in continuous operation during the field test, providing similar conditions for all three vertical flights. However, the emission plume had a particularly well-defined shape while performing the ascent at 12:08, and, as Figure 7a shows, it was moving towards the vertical path of the UAV platform. When comparing the picture from the flights with the corresponding wind rose during that ascent, shown in Figure 7b, it was confirmed that the data collected with the wind sensor agrees with the wind direction in the picture. The wind came predominantly from the east, with wind speed values mostly over 3 m/s, which might have favored the uniform transport of the emission plume.

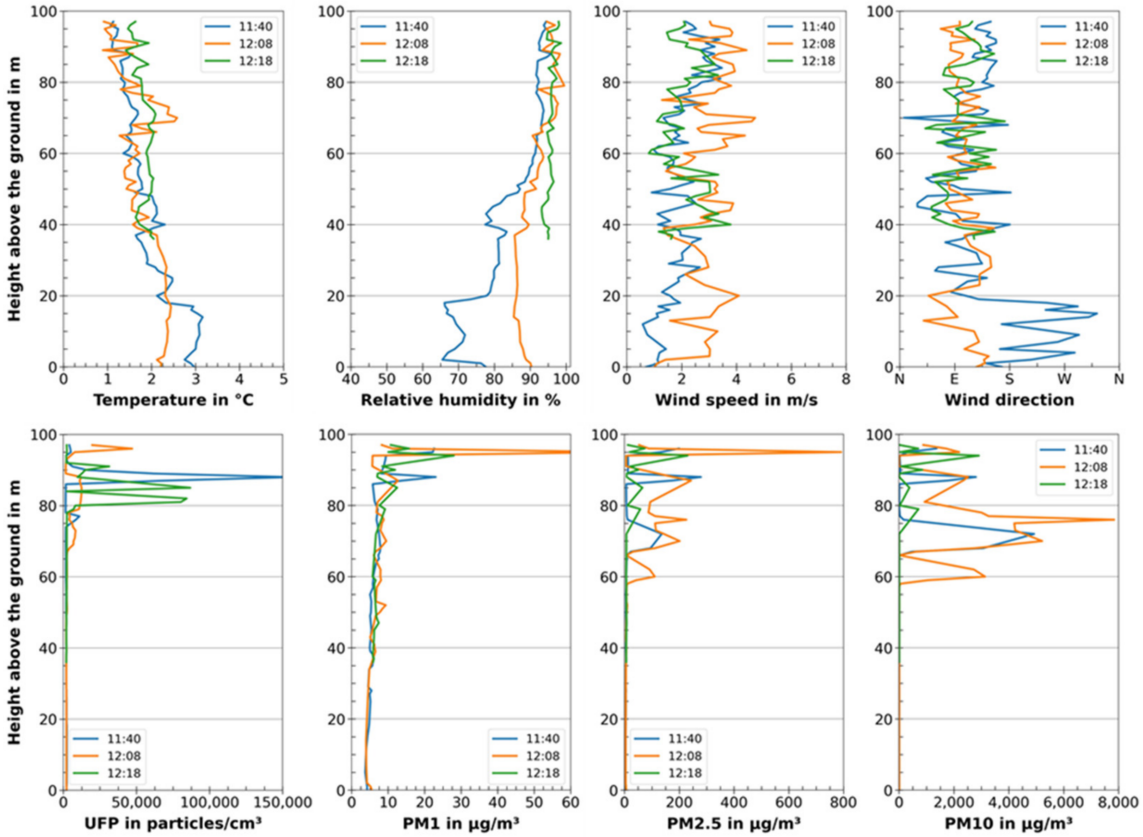


Figure 6. Vertical profiles of the meteorological parameters and air pollutants during the field test (ascents) on 31 January 2021.

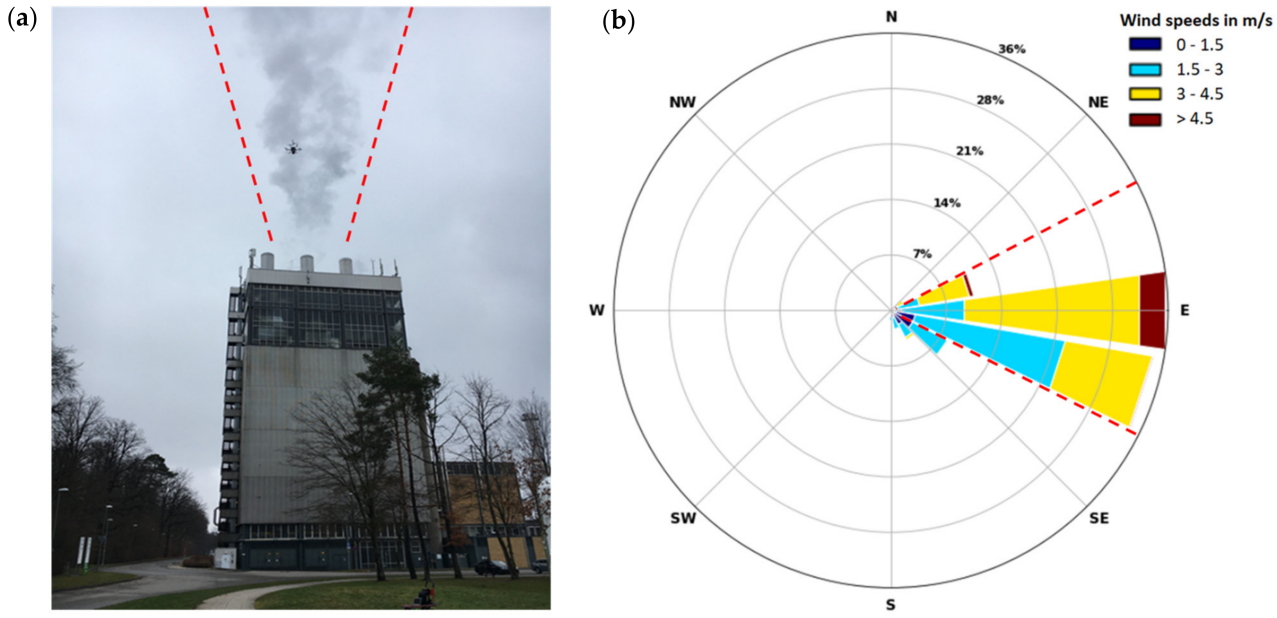


Figure 7. (**a**) Picture taken during the ascent at 12:08 local time and (**b**) wind rose showing the wind speed and wind direction measured with the TriSonica Mini during the same ascent on 31 January 2021.

For a more detailed analysis, the vertical profiles of the meteorological and pollutant parameters of the ascent at 12:08 local time are presented independently in Figure 8. The temperature profile shows an overall decrease with height and a sudden increase at heights

between 70 and 80 m, which might have been due to warmer emissions coming from the power plant. The relative humidity was high at the same height, reaching about 95%.

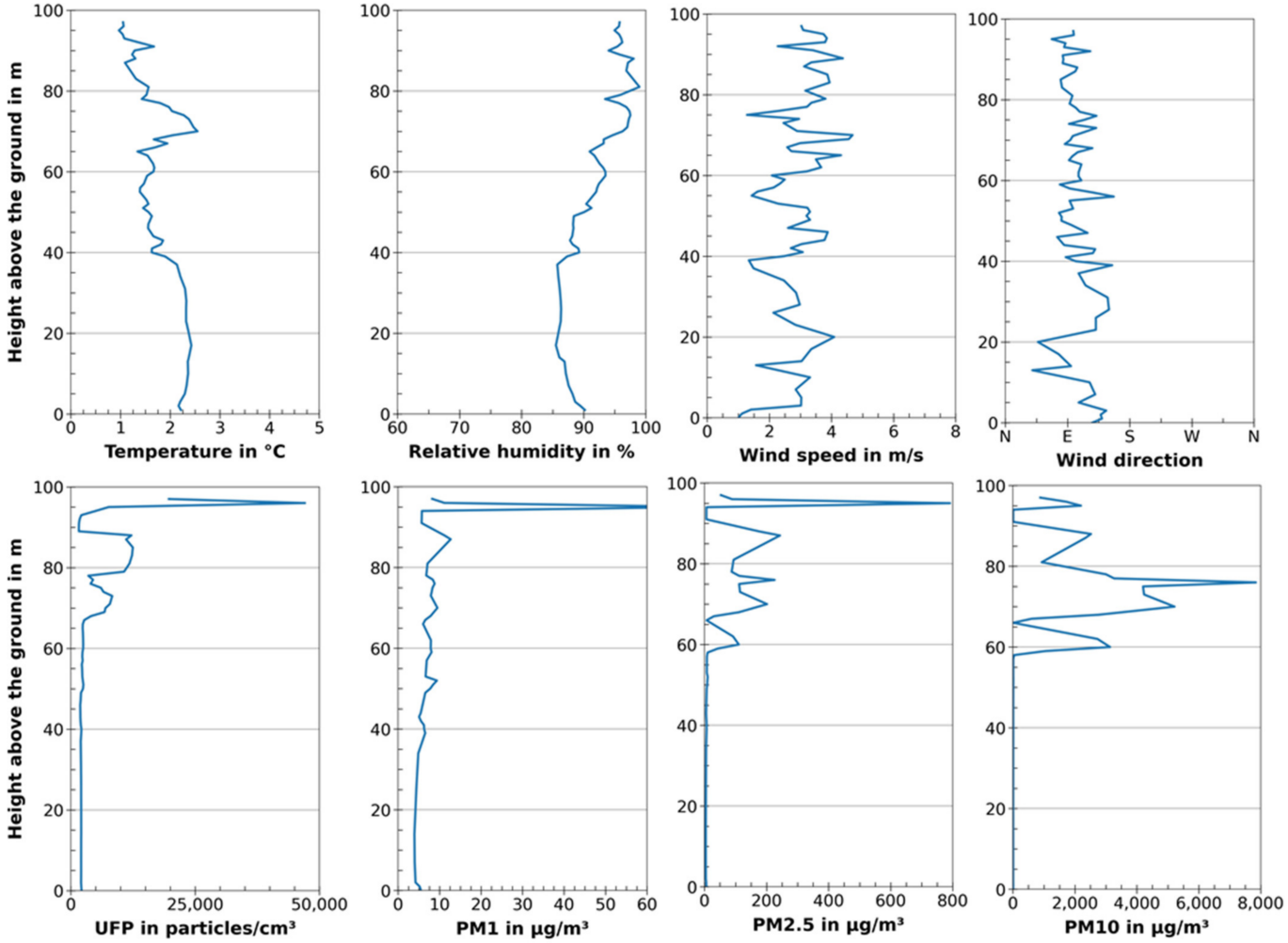


Figure 8. Vertical profiles of the meteorological parameters and air pollutants during the ascent at 12:08 local time on 31 January 2021.

The UFP profile shows nearly no variation in the concentrations at heights below 70 m, with values of about 2500 particles/cm^3. Above that height, the particle number concentrations started increasing, with the highest peak of about 45,000 particles/cm^3 at the height of 95 m. From the PM1 profile, it can be seen that a similar trend compared with the UFP profile. The concentrations remained almost constant from the ground up to the height of 40 m, with a value of 5 µg/m^3. Then, between the elevation of 40 and 80 m, the concentrations showed variations between 5 and 10 µg/m^3. Subsequently, between heights of 80 and 100 m, the concentrations further increased and reached a peak of about 60 µg/m^3 at the height of 95 m. These results suggest that the emission plume extended between the heights of 70 and 100 m during the ascent at 12:08. The PM2.5 profile also shows a similar trend. A significant concentration increase of nearly 100 µg/m^3 was measured at a height of 60 m, followed by two higher concentration peaks of approximately 300 µg/m^3 at the heights of 70 and 75 m. Then again, the largest peak, of about 800 µg/m^3, was observed at the height of 95 m. This indicates that bigger particles were measured at lower altitudes due to their weight. The PM10 profile backs up that assumption. The first significant concentration peak of around 3000 µg/m^3 was measured at a height of 60 m, but the largest concentration peaks of 5000 and nearly 8000 µg/m^3 were observed at the heights of 70 and 75 m, respectively. Then, the concentrations dropped and had two more peaks between the

heights of 80 and 100 m. Thus, the results from the PM2.5 and PM10 profiles imply that the emission plume, at a horizontal distance of about 60 m from the source, was vertically extended approximately 40 m between the heights of 60 and 100 m.

Figure 9 shows a three-dimensional visualization of PM1 and PM2.5 average concentrations during the three ascents performed during the field test. This result is plotted using QGIS software. The PM1 concentrations reached concentrations above 15 µg/m^3 at around 80 m from the ground and kept increasing up to the height of 100 m (Figure 9a), while the PM2.5 concentrations showed values higher than 30 µg/m^3 at heights between 60 and 100 m, as shown in Figure 9b. Both illustrations support the results analyzed in the vertical profiles from the ascent at 12:08 local time.

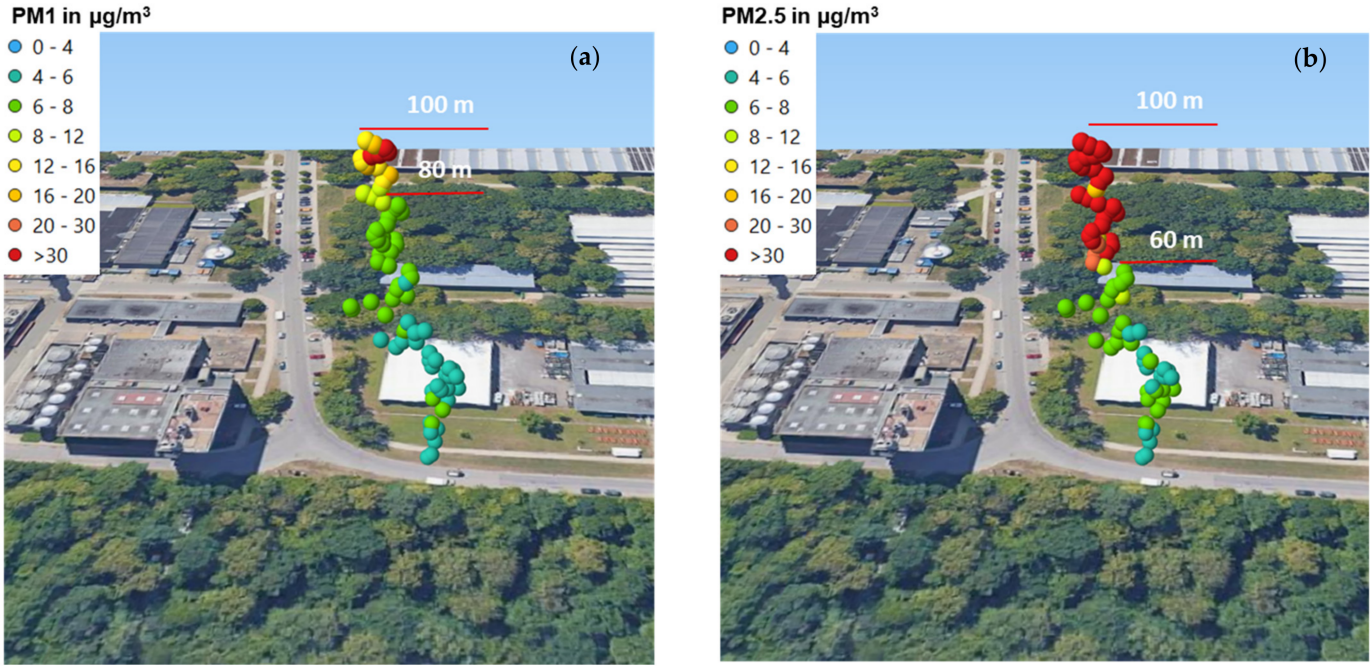


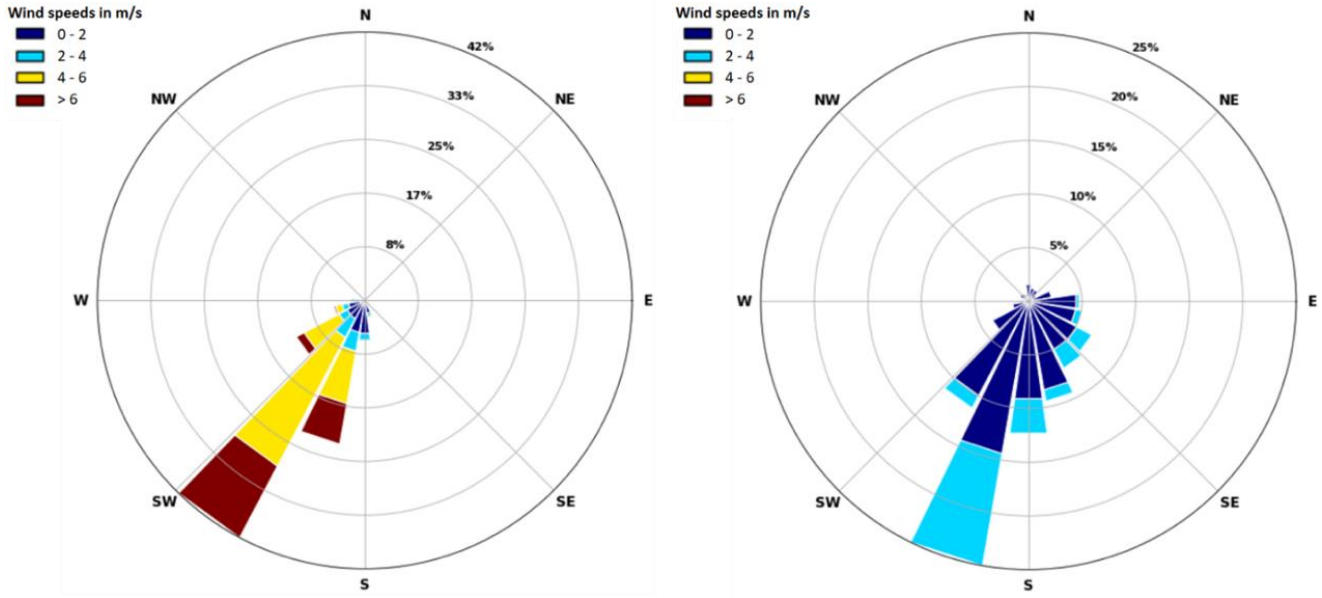
Figure 9. Three-dimensional visualization of the average concentrations of (**a**) PM1 and (**b**) PM2.5 during the three ascents performed in the field test on 23 January 2021.

4.2. Measurement Campaign Results

The wind rose graphs in Figure 10a,b illustrate the wind data measured with the TriSonica Mini for the time period of the vertical flights performed on 16 and 19 January 2021, respectively. On 16 January 2021, the wind speed values were mostly higher than 4 m/s and the wind direction was predominantly from the southwest. By contrast, on 23 January 2021, the wind speed values were lower than 4 m/s and the wind mainly came from the southwest and the south (see Section 4.3 Horizontal Measurements). Those conditions were suitable for the purpose of this study, as the traffic emissions were being transported towards the area where the measurements were conducted.

Figure 11 shows the vertical profiles of the meteorological parameters and air pollutants during the flight performed at 13:52 on 16 January 2021; the blue line represents the ascent and the orange line the descent. The temperature profile shows a uniform decrease with altitude and a total drop of 1 °C from the ground up to the height of 120 m. The relative humidity was nearly constant, at about 60%. The wind speed was relatively low up to a height of around 20 m and gradually increased with altitude, reaching values of up to 7 m/s. The wind direction was consistently from the south and the southwest. The BC and UFP concentrations slightly decreased with altitude and the average values for the complete flight were 0.6 µg/m^3 or 600 ng/m^3 and 5600 particles/cm^3, respectively. Overall, there was a well-mixed atmosphere from the ground up to 120 m AGL, which

can be attributed to the relatively high horizontal wind speeds with an average value of 4.6 m/s.



(**a**) (**b**)

Figure 10. Wind rose graphs showing wind speed and wind direction measured with the TriSonica Mini for the time of the vertical flights made on (**a**) 16 January 2021 and (**b**) 19 January 2021.

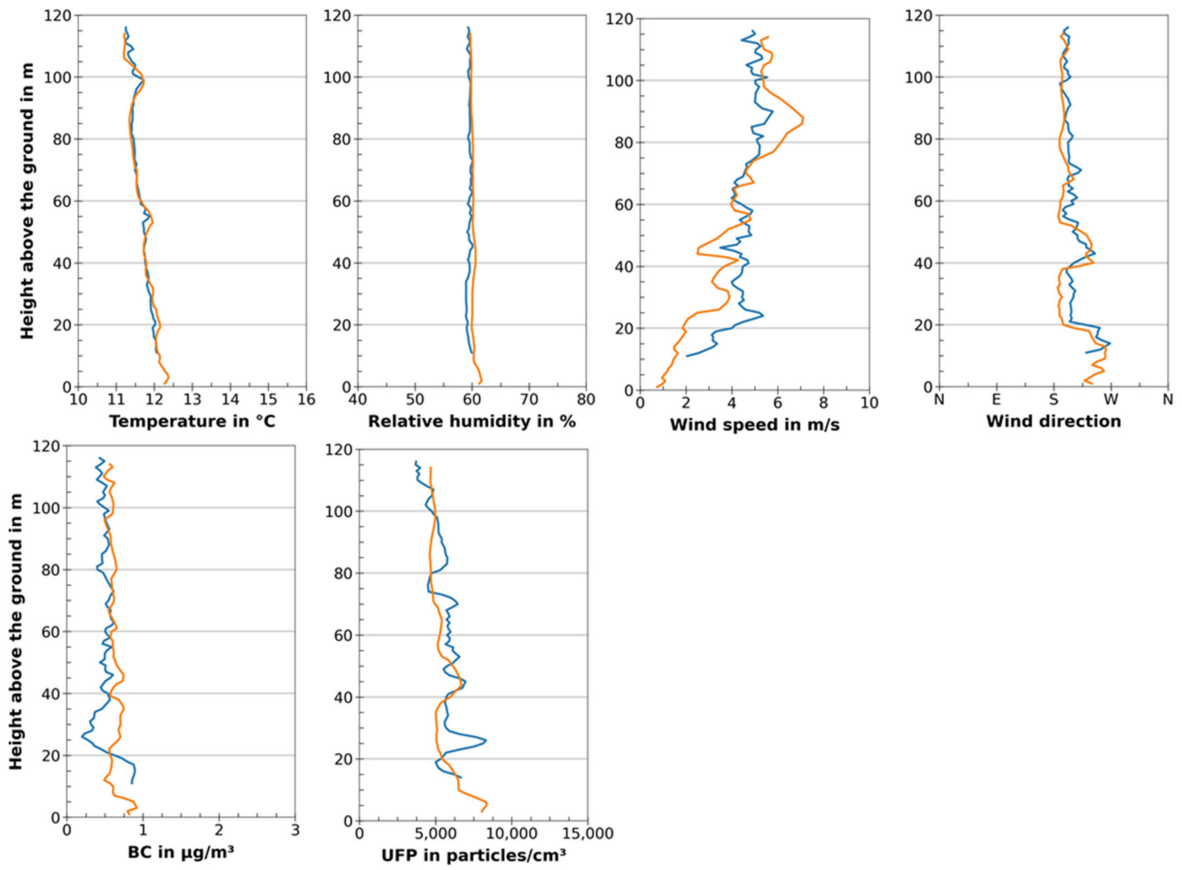


Figure 11. Vertical profiles (ascent: blue line; descent: orange line) of the meteorological parameters and air pollutants during the flight at 13:52 local time on 16 January 2021.

Figure 12 shows the vertical profiles of the meteorological parameters and air pollutants during the flight performed at 11:14 local time on 23 January 2021; the blue line represents the ascent and the orange line the descent. The temperature profile showed a similar trend to that of 16 January 2021, decreasing with altitude and without an inversion layer. There was a total drop of 2 °C from the ground up to the culmination point, which is most clearly seen during the descent. The ascent shows more fluctuation, which can be attributed to preheating of the plastic housing containing the sensor due to the strong solar radiation on 23 January 2021. The wind speed profile shows the lowest values at the ground level, a pattern that was observed for all the wind speed profiles and which might have been due to the friction of a tree line located between the road and the take-off point. The average wind speed values were about 1.8 m/s, considerably lower than during the flight on 16 January 2021. The wind direction remained stable throughout the flight, between south and southwest.

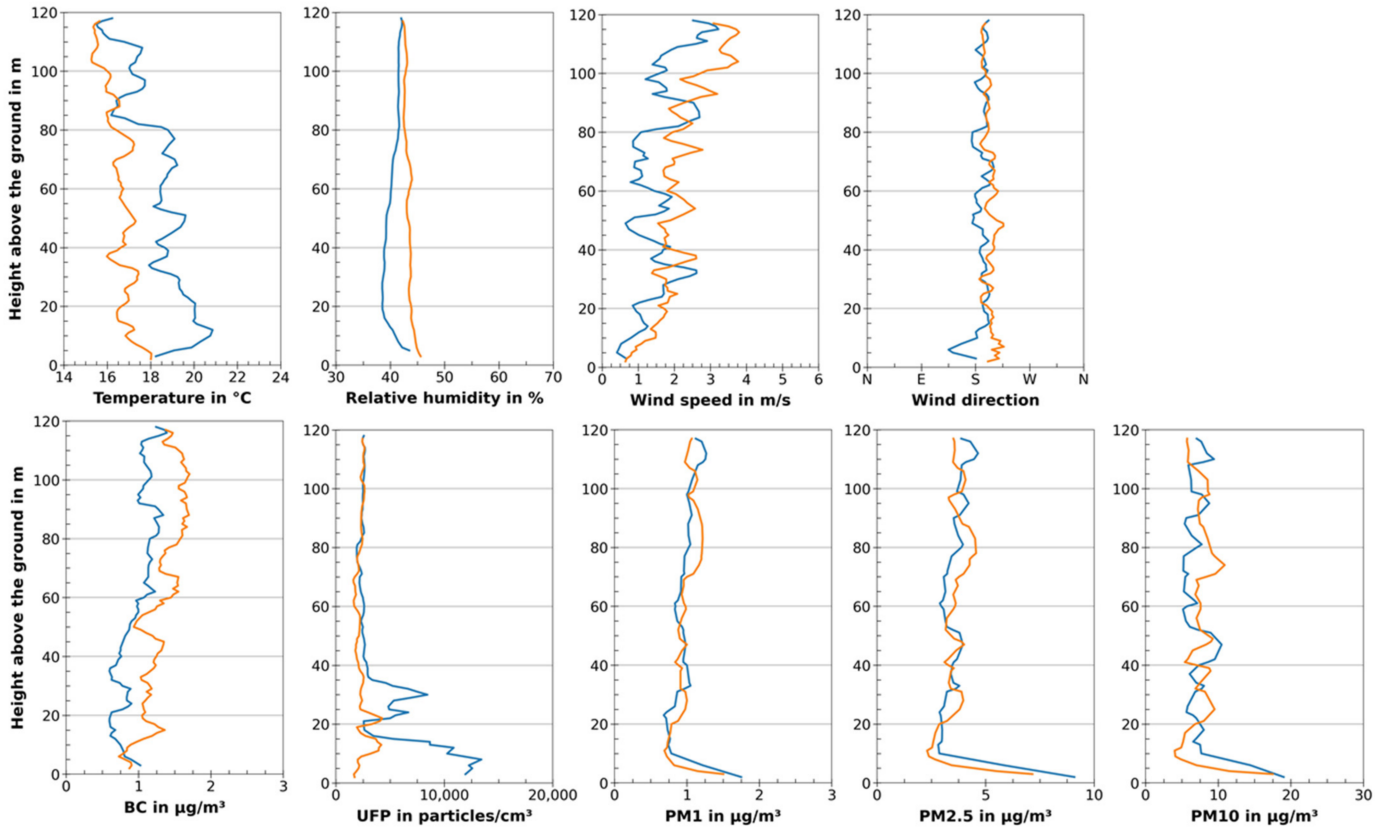


Figure 12. Vertical profiles (ascent: blue line; descent: orange line) of the meteorological parameters and air pollutants during the flight at 11:14 on 23 January 2021.

The BC concentrations, compared with the flight on 16 January 2021, were higher and slightly increased with altitude. The average BC concentration was 1.13 µg/m^3. The UFP concentrations showed fluctuations from the ground up to a height of 40 m, with the highest values around 13,000 particles/cm^3 at a height of 10 m. After the height of 40 m, there was a uniform distribution with an average concentration of 2100 particles/cm^3. PM concentration profiles followed a similar trend—higher concentrations on the ground and an immediate reduction during the first few meters. Above the 10 m height, the concentrations were consistently distributed throughout the flight. PM1, PM2.5, and PM10 measured on the ground were about 1.6 µg/m^3, 8 µg/m^3, and 19 µg/m^3, respectively, and the average values of the complete flight were about 1 µg/m^3, 3.6 µg/m^3, and 7.5 µg/m^3, respectively. On 23 January 2021, wind speed values were relatively low, in the range of about 2 m/s. However, it was a clear sunny day with strong solar radiation, which

could have favored the convection of air masses, resulting in a good vertical mixing of the pollutants.

4.3. Horizontal Measurements

Two horizontal flights were made, moving in a parallel and perpendicular direction to the federal highway B14 for about 100 m and 50 m, respectively, at a height of 30 m AGL. The flights were carried out carefully maintaining a constant speed of approximately 1 m/s and avoiding the rotation of the UAV platform.

The wind rose graph in Figure 13 illustrates the wind data measured with the TriSonica Mini for the duration of the horizontal flight at 13:41 on 23 January 2021. The wind speed varied between 1 and 4 m/s, and the wind direction was mainly from the southeast, which was convenient for the measurements that were being made. Figures 14 and 15 show the three-dimensional visualization of the concentrations of UFP and PM10, respectively, measured during the horizontal flight at 13:41 local time on 23 January 2021. Both graphs show that at a height of 30 m, the concentrations were higher at the roadside and decreased with increasing distance from the road.

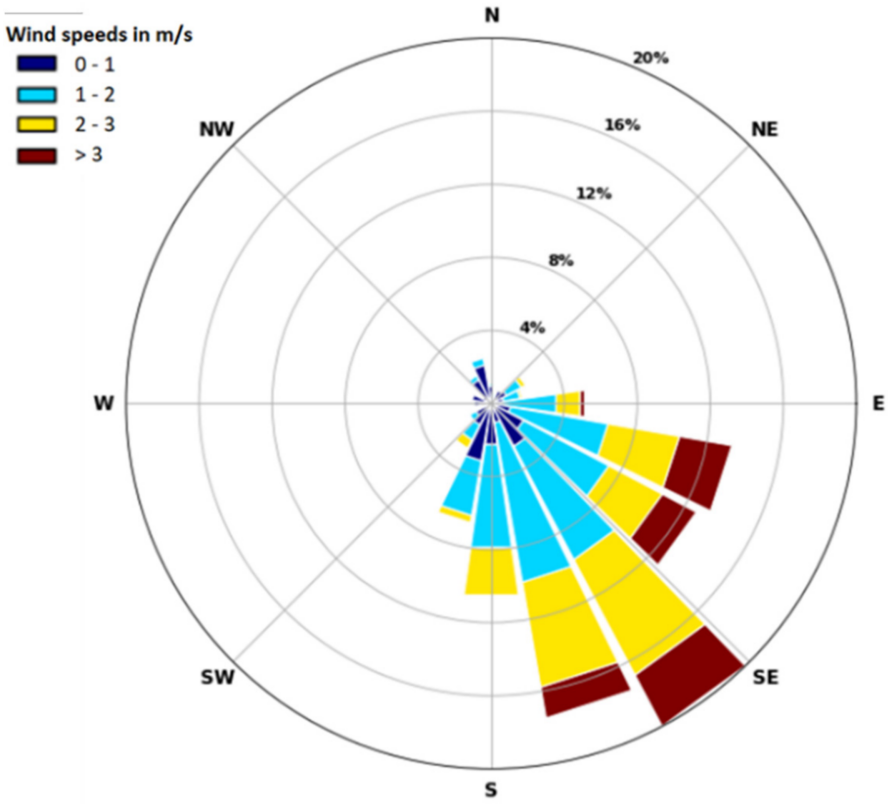


Figure 13. Wind rose showing the wind speed and wind direction measured with the TriSonica Mini during the horizontal flight performed at 13:41 local time on 23 January 2021.



Figure 14. Three-dimensional visualization of the UFP concentrations measured with the DISCmini during the horizontal flight at 30 m AGL performed at 13:41 local time on 23 January 2021.

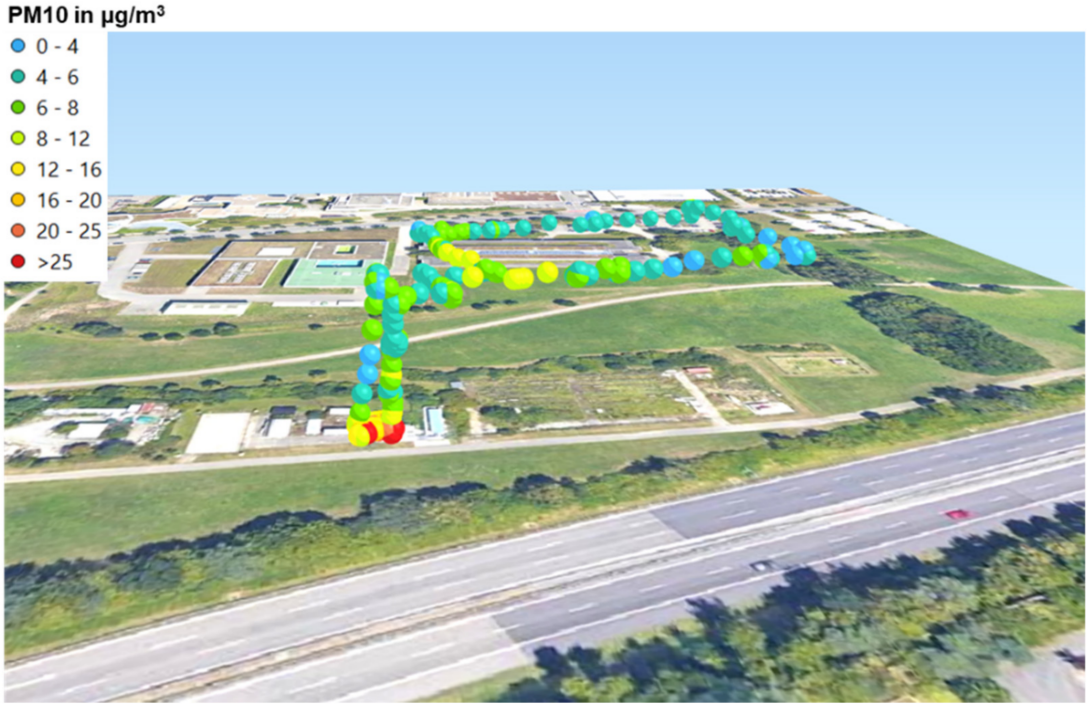


Figure 15. Three-dimensional visualization of the PM10 concentrations measured with the OPC-N3 during the horizontal flight at 30 m AGL performed at 13:41 on 23 January 2021.

5. Quality Assurance

Quality assurance was obtained for all the portable sensors and devices by comparing them with reference instruments. The aethalometer AE51 used in this study was validated with its most recent version from the same company (AethLabs), the aethalometer MA200 (reference instrument). The comparison between the two devices was carried out in the

laboratory for about 3 h, using a flow rate of 150 mL/min. After checking the average BC values in µg/m^3 measured by the two aethalometers, a minor offset was found between the two devices. A simple linear regression was applied to correct the AE51 data according to the MA200 device. The comparison results for these two devices are shown in Figure 16. The curves from both devices correspond to each other and the results are comparable. The Diffusion Charger DISCmini (DC#1) used in this study was compared with another DISCmini (DC#2) from the same company (Testo). Figure 17 shows the comparison between the two devices. Since the DC#1 was newer and more recently calibrated by the manufacturing company, it was selected as the reference device to which the results of the second instrument were related. Since there was no significant deviation between the two devices, no corrections were applied to this data. The OPC-N3 used in the present study was compared with a Grimm model EDM 180. The parallel measurements were conducted over a period of three days at the air quality monitoring station located at Marienplatz in Stuttgart. Figure 18 shows the average PM2.5 min values measured by the two instruments. Both graphs showed a similar trend, but there were some small inconsistent gaps between them that may have been due to the susceptibility of OPC-N3 to relative humidity. Therefore, no correction was performed on the raw data obtained.

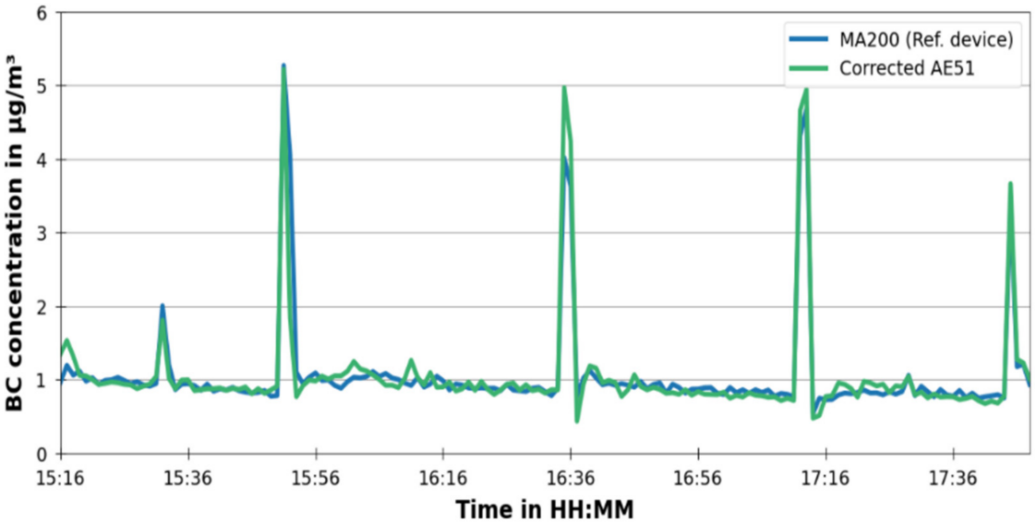


Figure 16. Comparison between the reference device data (MA200) and the corrected data (AE51).

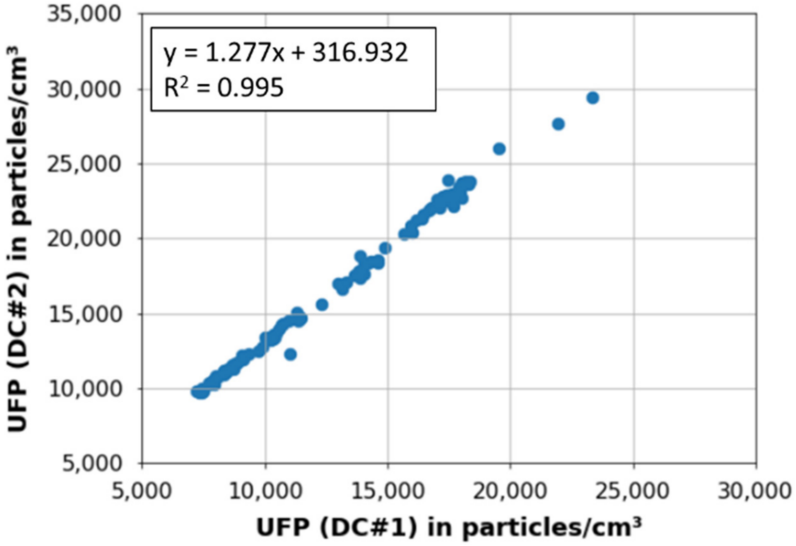


Figure 17. Comparison of the UFP device (DC#2) with the reference device (DC#1).

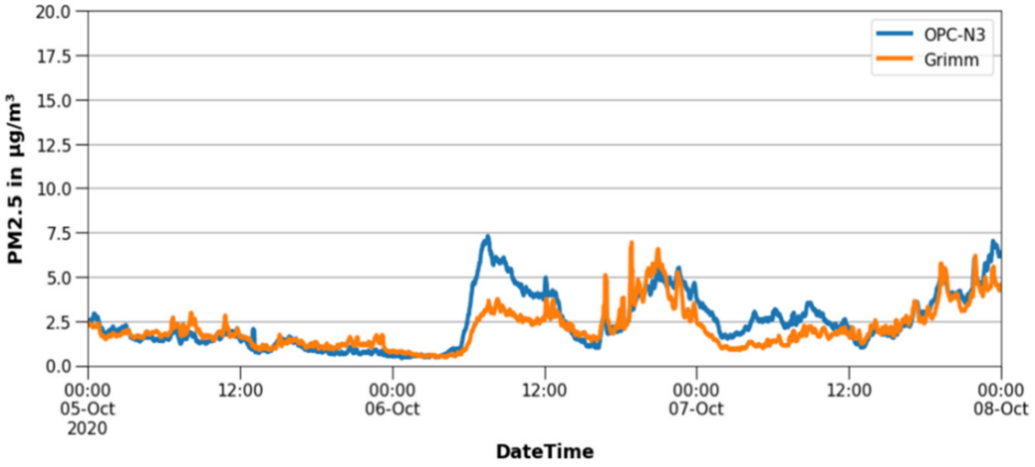


Figure 18. Average minute values for PM2.5 comparison from the two OPCs.

The atmospheric sensors were compared with the Compact Weather Station MaxiMet GILL. The parallel measurements were carried out over a period of four days. Figure 19 a–c shows the comparison of the air temperature, air pressure, and relative humidity data respectively obtained with the two devices. The results obtained showed good agreement between the sensor and the reference device. Therefore, no correction was applied to the temperature and pressure raw data from the iMet-XQ2. The average relative humidity values measured by the two atmospheric sensors showed a similar trend. However, there was an offset between the two devices which was corrected during the evaluation.

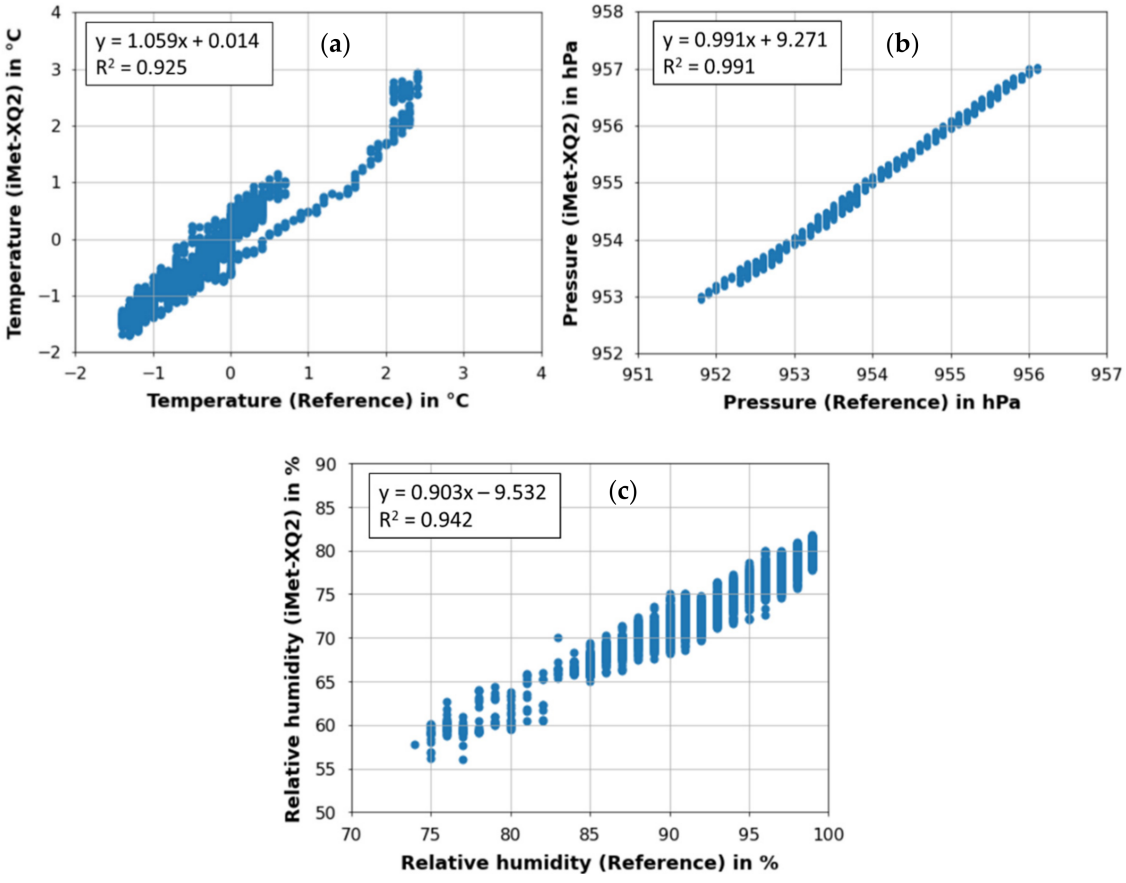


Figure 19. Comparison of (**a**) air temperature, (**b**) air pressure, and (**c**) relative humidity results (iMet-XQ2) with the reference device (GILL).

6. Conclusions

The UAV platform developed for air quality monitoring presented in this study was based on a multi-rotor UAV with high flight performance and payload capabilities equipped with lightweight precise sensors. The experiments have shown that the UAV platform is stable, safe to operate, and capable of performing high-resolution three-dimensional measurements of particulate matter, ultrafine particles, black carbon, and meteorological parameters. This 14 kg UAV platform had a flight time of around 15 min and a low operating cost. It can be easily assembled and disassembled, facilitating transport to measurement sites and reducing setup time, making it a practical, cost-effective instrument for air quality monitoring near a source. However, a stable communication signal between the hexacopter UAV and remote controller has to be guaranteed at all times.

The visual smoke test revealed that the optimal height for the sensor air inlets and the wind sensor was 90 cm above the selected hexacopter UAV propeller level. Below that, the vertical airflows caused by the propellers had an influence on the measurements, the magnitude of which increases as the distance between the propellers and the plume of smoke passing over the hexacopter UAV is reduced.

Three different vertical flight paths were performed during the measurement campaign. The results have shown that the UAV can perform reliable measurements while ascending and descending, and the suggested flight path includes 10 s hovering every 10 m in order to obtain more representative data. The method of obtaining vertical profiles and horizontal profiles above the ground with the UAV platform provided a good overview to study the distribution of pollutants in the atmosphere. The field test profiles showed the potential of the UAV platform to assess the extent and scope of industrial emission plumes. The case study profiles confirmed that traffic-induced emissions were higher near the roads but dropped to background levels with increasing distance vertically or horizontally. In addition, the measurements have shown that the meteorological parameters influenced the pollutant concentrations directly. High wind speeds helped the pollutants to disperse quickly, and strong solar radiation favored the convection of air masses, resulting in good vertical mixing of the pollutants.

In the end, it can be concluded that the UAV platform developed by the authors is suitable for horizontal and vertical profile measurements and that it provided substantial information regarding the air quality near the ground up to a certain height.

Author Contributions: Conceptualization, A.S., D.A.F., I.C. and U.V.; methodology, A.S., D.A.F., I.C. and U.V.; software, A.S., D.A.F. and I.C.; validation, A.S., D.A.F. and I.C.; formal analysis, A.S., D.A.F. and I.C.; investigation, A.S., D.A.F. and I.C.; resources, U.V.; data curation, A.S., D.A.F. and I.C.; writing—original draft preparation, A.S. and D.A.F.; writing—review and editing, A.S., D.A.F., I.C. and U.V.; visualization, A.S., D.A.F. and I.C.; supervision, A.S., I.C. and U.V.; project administration, A.S., I.C. and U.V.; funding acquisition, U.V. All authors have read and agreed to the published version of the manuscript.

Funding: This research received no external funding.

Institutional Review Board Statement: Not applicable.

Informed Consent Statement: Not applicable.

Data Availability Statement: The data presented in this study are available on request from the corresponding author.

Conflicts of Interest: The authors declare no conflict of interest.

References

1. European Environment Agency. *Air Quality in Europe: 2019 Report*; Publications Office, European Environment Agency: Copenhagen, Denmark, 2019.
2. Health Effects Institute. Traffic-Related Air Pollution: A Critical Review of the Literature on Emissions, Exposure, and Health Effects. In *HEI Special Report 17*; HEI: Boston, MA, USA, 2010.

3. Samad, A.; Vogt, U. Investigation of urban air quality by performing mobile measurements using a bicycle (MOBAIR). *Urban Clim.* **2020**, *33*, 100650. [CrossRef]
4. Durant, J.L.; Ash, C.A.; Wood, E.C.; Herndon, S.C.; Jayne, J.T.; Knighton, W.B.; Canagaratna, M.R.; Trull, J.B.; Brugge, D.; Zamore, W.; et al. Short-term variation in near-highway air pollutant gradients on a winter morning. *Atmos. Chem. Phys.* **2010**, *10*, 8341–8352. [CrossRef]
5. Villa, T.F.; Gonzalez, F.; Miljievic, B.; Ristovski, Z.D.; Morawska, L. An Overview of Small Unmanned Aerial Vehicles for Air Quality Measurements: Present Applications and Future Prospectives. *Sensors* **2016**, *16*, 1072. [CrossRef] [PubMed]
6. Villa, T.F.; Salimi, F.; Morton, K.; Morawska, L.; Gonzalez, F. Development and Validation of a UAV Based System for Air Pollution Measurements. *Sensors* **2016**, *16*, 2202. [CrossRef]
7. Cao, R.; Li, B.; Wang, H.-W.; Tao, S.; Peng, Z.-R.; He, H. Vertical and Horizontal Profiles of Particulate Matter and Black Carbon Near Elevated Highways Based on Unmanned Aerial Vehicle Monitoring. *Sustainability* **2020**, *12*, 1204. [CrossRef]
8. Samad, A.; Vogt, U.; Panta, A.; Uprety, D. Vertical distribution of particulate matter, black carbon and ultra-fine particles in Stuttgart, Germany. *Atmos. Pollut. Res.* **2020**, *11*, 1441–1450. [CrossRef]
9. Gu, Q.; Michanowicz, D.R.; Jia, C. Developing a Modular Unmanned Aerial Vehicle (UAV) Platform for Air Pollution Profiling. *Sensors* **2018**, *18*, 4363. [CrossRef] [PubMed]
10. Villa, T.F.; Jayaratne, E.R.; Gonzalez, L.F.; Morawska, L. Determination of the vertical profile of particle number concentration adjacent to a motorway using an unmanned aerial vehicle. *Environ. Pollut.* **2017**, *230*, 134–142. [CrossRef]
11. Chiliński, M.T.; Markowicz, K.M.; Kubicki, M. UAS as a Support for Atmospheric Aerosols Research: Case Study. *Pure Appl. Geophys.* **2018**, *175*, 3325–3342. [CrossRef]
12. Zhu, Y.; Wu, Z.; Park, Y.; Fan, X.; Bai, D.; Zong, P.; Qin, B.; Cai, X.; Ahn, K.-H. Measurements of atmospheric aerosol vertical distribution above North China Plain using hexacopter. *Sci. Total Environ.* **2019**, *665*, 1095–1102. [CrossRef] [PubMed]
13. Liu, B.; Wu, C.; Ma, N.; Chen, Q.; Li, Y.; Ye, J.; Martin, S.T.; Li, Y.J. Vertical profiling of fine particulate matter and black carbon by using unmanned aerial vehicle in Macau, China. *Sci. Total Environ.* **2020**, *709*, 136109. [CrossRef] [PubMed]
14. Zheng, Y.; Yang, S.; Liu, X.; Wang, J.; Norton, T.; Chen, J.; Tan, Y. The computational fluid dynamic modeling of downwash flow field for a six-rotor UAV. *Front. Agric. Sci. Eng.* **2018**, *5*, 159–167. [CrossRef]
15. Crazzolara, C.; Ebner, M.; Platis, A.; Miranda, T.; Bange, J.; Junginger, A. A new multicopter-based unmanned aerial system for pollen and spores collection in the atmospheric boundary layer. *Atmos. Meas. Tech.* **2019**, *12*, 1581–1598. [CrossRef]
16. Li, B.; Cao, R.; Wang, Z.; Song, R.-F.; Peng, Z.-R.; Xiu, G.; Fu, Q. Use of Multi-Rotor Unmanned Aerial Vehicles for Fine-Grained Roadside Air Pollution Monitoring. *Transp. Res. Rec. J. Transp. Res. Board* **2019**, *2673*, 169–180. [CrossRef]
17. De Fazio, R.; Dinoi, L.M.; De Vittorio, M.; Visconti, P.A. Sensor-Based Drone for Pollutants Detection in Eco-Friendly Cities: Hardware Design and Data Analysis Application. *Electronics* **2022**, *11*, 52. [CrossRef]
18. Pochwała, S.; Anweiler, S.; Deptuła, A.; Gardecki, A.; Lewandowski, P.; Przysiężniuk, D. Optimization of air pollution measurements with unmanned aerial vehicle low-cost sensor based on an inductive knowledge management method. *Optim. Eng.* **2021**, *22*, 1783–1805. [CrossRef]
19. Alvear, O.; Zema, N.R.; Natalizio, E.; Calafate, C.T. Using UAV-Based Systems to Monitor Air Pollution in Areas with Poor Accessibility. *J. Adv. Transp.* **2017**, *2017*, 8204353. [CrossRef]
20. Jumaah, H.J.; Kalantar, B.; Halin, A.A.; Mansor, S.; Ueda, N.; Jumaah, S.J. Development of UAV-Based PM2.5 Monitoring System. *Drones* **2021**, *5*, 60. [CrossRef]
21. Alphasense Ltd. Alphasense User Manual OPC-N3 Optical Particle Counter. 2019. Available online: https://www.alphasense.com/wp-content/uploads/2019/03/OPC-N3.pdf (accessed on 9 February 2022).
22. Testo DISCmini. Testo-DiSCmini-Instruction-Manual, 8–10. 2016. Available online: https://static-int.testo.com/media/e6/b0/b0ea52f6be7a/testo-DiSCmini-Instruction-manual.pdf (accessed on 9 February 2022).
23. AethLabs. MicroAeth AE51 Operating Manual, 6. 2016. Available online: https://aethlabs.com/sites/all/content/microaeth/ae51/microAeth%20AE51%20Operating%20Manual%20Rev%2006%20Updated%20Jul%202016.pdf (accessed on 9 February 2022).
24. Mide Technology Corporation. Air Pressure at Altitude Calculator. 2021. Available online: https://www.mide.com/air-pressure-at-altitude-calculator (accessed on 1 February 2021).